Correlation-Induced Triplet Pairing Superconductivity in Graphene-Based Moiré Systems

Yang-Zhi Chou,[1,*] Fengcheng Wu,[2] Jay D. Sau,[1] and Sankar Das Sarma[1]
[1]*Condensed Matter Theory Center and Joint Quantum Institute, Department of Physics, University of Maryland, College Park, Maryland 20742, USA*
[2]*School of Physics and Technology, Wuhan University, Wuhan 430072, China*

(Received 8 May 2021; accepted 12 October 2021; published 15 November 2021)

Motivated by the possible non-spin-singlet superconductivity in the magic-angle twisted trilayer graphene experiment, we investigate the triplet-pairing superconductivity arising from a correlation-induced spin-fermion model of Dirac fermions with spin, valley, and sublattice degrees of freedom. We find that the f-wave pairing is favored due to the valley-sublattice structure, and the superconducting state is time-reversal symmetric, fully gapped, and nontopological. With a small in-plane magnetic field, the superconducting state becomes partially polarized, and the transition temperature can be slightly enhanced. Our results apply qualitatively to Dirac fermions for the triplet-pairing superconductivity in graphene-based moiré systems, which is fundamentally distinct from triplet superconductivity in ^{3}He and ferromagnetic superconductors.

DOI: 10.1103/PhysRevLett.127.217001

Introduction.—Since the incipient discovery of correlated insulators and superconductivity in magic-angle twisted bilayer graphene (MATBG) [1,2], the moiré graphene systems continue to uncover exotic phases and excite new ideas [3–21]. In particular, magic-angle twisted trilayer graphene (MATTG) [19–21] establishes a second example of the robust superconductivity in the moiré graphene systems that reveals a clear Fraunhofer-like oscillation in a Josephson interference pattern. In addition, the out-of-plane displacement field can modify the band structure significantly, providing a controllable way to tune the Van Hove singularity as well as the superconductivity [19–21].

A recent experiment in MATTG [21] demonstrated that the superconducting state survives with a large in-plane magnetic field (until ∼10 T) that exceeds the Pauli limit for spin-singlet superconductivity, *prima facie* implying a non-spin-singlet superconducting state in MATTG. Remarkably, the experiment also found a nonmonotonic superconducting behavior as a function of the applied in-plane magnetic field, which suggests a separate (reentrant) superconducting phase for magnetic field beyond 8 T.

In this Letter, we study a spin-fermion model [22–27] for Dirac fermions with spin, valley, and sublattice degrees of freedom, as a proxy for investigating the possible spin-triplet superconductivity in graphene-based moiré systems. The idea is that the system is proximate to correlation-induced ferromagnetism even when the long-ranged order is not observed. The fluctuation of such a phase (i.e., spin fluctuation) is captured by the spin-fermion model, and the spin fluctuation generates superconductivity regardless of the details in the band structure. We establish that the spin-triplet superconducting state is f wave [see Fig. 1(a)] and fully gapped due to the valley-sublattice structure in the Cooper pairs. We also discuss the effect of a small in-plane magnetic field and experimental characterization.

We note that the sublattice and valley structures in the pairing states crucially determine the dominating pairing instability, while the moiré band structures in twisted graphene systems inherit Dirac fermions with internal degrees of freedom (e.g., spin, valley, sublattice) from monolayer graphene. Therefore, we anticipate that the f wave is generically the dominating pairing symmetry for spin-triplet superconductivity in the graphene based systems.

Model.—The spin-fermion model [22–27] describes that the low-energy itinerant electrons interact with the fluctuating *spin fields*. Although the spin fields arise from the electrons microscopically, we treat them as independent

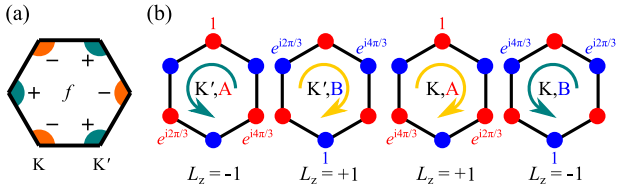

FIG. 1. (a) f-wave pairing symmetry and the Brillouin zone. The signs indicate the relative phase when an f-wave pairing is rotated by $\pi/3$. K and K' denote the valleys. (b) Angular momentum and valley-sublattice structure. The electrons carry finite angular momenta depending on the valley and sublattice as depicted in the figure. Therefore, the Cooper pair wave function might carry nontrivial z-directional angular momentum (L_z). A and B denote the sublattices.

degrees of freedom in the spirit of the spin-fermion model [27]. In this work, we consider a spin-fermion model of Dirac fermions which can be realized on a honeycomb lattice, $\hat{H} = \hat{H}_e + \hat{H}_s + \hat{H}_{es}$. The low-energy electron is described by [28]

$$\hat{H}_e = \sum_{\mathbf{k}} \psi^\dagger_{\mathbf{k}} h_{\mathbf{k}} \psi_{\mathbf{k}}, \tag{1}$$

where

$$h_{\mathbf{k}} = \hbar v_F \sigma^x \tau^z k_x + \hbar v_F \sigma^y k_y - E_F. \tag{2}$$

In the above expression, σ^a (τ^a) denotes the a component of the Pauli matrices for the sublattice (valley), v_F is the Dirac velocity, E_F is the Fermi energy, and $\psi_{\mathbf{k}}$ is an eight-component fermionic field (valley, sublattice, and the *intrinsic* spin) with momentum $\mathbf{k}$. The reduced Hamiltonian $h_{\mathbf{k}}$ obeys a ($\mathcal{T}^2 = 1$) time-reversal operator, $\hat{\Pi} h^*_{-\mathbf{k}} \hat{\Pi}^{-1} = h_{\mathbf{k}}$, where $\hat{\Pi} = \tau^x$. The fluctuating spin fields are described by

$$\hat{H}_s = \frac{1}{2} \sum_{\mathbf{q}} \chi^{-1}(\mathbf{q}) \vec{S}_{-\mathbf{q}} \cdot \vec{S}_{\mathbf{q}}, \tag{3}$$

where $\chi^{-1}(\mathbf{q})$ is the inverse spin-spin zero-frequency correlation function and $\vec{S}_{\mathbf{q}} = (S^x_{\mathbf{q}}, S^y_{\mathbf{q}}, S^z_{\mathbf{q}})$ encodes the three-component fluctuating bosonic spin field at momentum $\mathbf{q}$. Finally, the spin-fermion coupling is given by

$$\hat{H}_{es} = \frac{g}{\sqrt{A}} \sum_{\mathbf{k},\mathbf{q}} \left(\psi^\dagger_{\mathbf{k}-\mathbf{q}} \frac{\vec{\mu}}{2} \psi_{\mathbf{k}} \right) \cdot \vec{S}_{\mathbf{q}}, \tag{4}$$

where g is the spin-fermion coupling constant, A is the area of the system, and the Pauli matrices for the spin $\vec{\mu} = (\mu^x, \mu^y, \mu^z)$. The spin-fermion model here is motivated by the non-spin-singlet superconductivity in the MATTG experiment near $\nu = -2$ [21] since spin fluctuation provides a natural explanation for the spin triplet pairing [29,30]. We further assume that the fluctuating spin fields fail to develop a long range order at the temperatures of our interest, but the spin-spin correlation function $\chi(\mathbf{q})$ is peaked at $\mathbf{q} = 0$, e.g., $\chi(\mathbf{q}) = \chi_0/(|\mathbf{q}|^2 + \xi^{-2})$ where $\chi_0 > 0$ and ξ is the correlation length. Such an assumption is consistent with the absence of ground state magnetization in MATTG experiment near $\nu = -2$ [21].

To obtain an effective interelectron interaction, we integrate out the fluctuating spin fields in Eqs. (3) and (4). The effective interaction is given by

$$\hat{H}_I = -\frac{g^2}{2A} \sum_{\mathbf{k},\mathbf{k}',\mathbf{q}} \chi(\mathbf{q}) \left(\psi^\dagger_{\mathbf{k}+\mathbf{q}} \frac{\vec{\mu}}{2} \psi_{\mathbf{k}} \right) \cdot \left(\psi^\dagger_{\mathbf{k}'-\mathbf{q}} \frac{\vec{\mu}}{2} \psi_{\mathbf{k}'} \right). \tag{5}$$

$\hat{H}_I$ describes the ferromagnetic interaction between the intrinsic spins of the itinerant electrons which favors spin-triplet pairing [29–31]. One possibility is paramagnon mediated interactions.

Pairing symmetry.—Besides the spin degrees of freedom, the valley and sublattice structures play important roles in the pairing symmetry of the superconductivity [32,33]. We discuss only the intervalley Cooper pairs as the intravalley Cooper pairs correspond to a lattice-scale oscillating gap function in the position space. The s wave and f-wave pairings are intrasublattice while the p wave and d-wave pairings are intersublattice [33]. To see this, we consider Cooper pairs in the position space and examine the symmetry operations in the following. The wave function under the threefold rotation ($\mathcal{C}_{3z}$) about a hexagon center is given by $\mathcal{C}_{3z}\psi^\dagger(\mathbf{r})\mathcal{C}^{-1}_{3z} = e^{i(2\pi/3)\tau_z\sigma_z}\psi^\dagger(\mathcal{R}_3\mathbf{r})$ because of the site-dependent Bloch wave phase factors illustrated in Fig. 1(b). In addition, the twofold rotation ($\mathcal{C}_{2z}$) about a hexagon center is implemented by the valley and sublattice exchanging as follows: $\mathcal{C}_{2z}\psi^\dagger(\mathbf{r})\mathcal{C}^{-1}_{2z} = \tau^x\sigma^x\psi^\dagger(\mathcal{R}_2\mathbf{r})$. For a pair of electrons from different valleys, $\mathcal{C}_{3z}$ operation can distinguish the s wave and f wave ($L_z \bmod 3 = 0$) from the p wave and d wave ($L_z \bmod 3 = 1, 2$); $\mathcal{C}_{2z}$ operation can distinguish the s wave and d wave ($L_z \bmod 2 = 0$) from the p wave and f wave ($L_z \bmod 2 = 1$). With both $\mathcal{C}_{3z}$ and $\mathcal{C}_{2z}$, we can classify angular momentum states associated with $|L_z| = 0, 1, 2, 3$. Therefore, the sublattice structures are fully determined for the intervalley s-, p-, d-, and f-wave pairings [32,33].

The spin-triplet Cooper pair bilinears are summarized in the following. (The spin-singlet operators are listed in Sec. I of [31].) The p-wave spin-triplet Cooper pairs are intersublattice and are given by

$$\vec{\Phi}_{p,X}(\mathbf{k}) = \psi^T_{-\mathbf{k}}[(-i\tau^y)\sigma^x(i\vec{\mu}\mu^y)^\dagger]\psi_{\mathbf{k}}, \tag{6}$$

$$\vec{\Phi}_{p,Y}(\mathbf{k}) = \psi^T_{-\mathbf{k}}[\tau^x(i\sigma^y)(i\vec{\mu}\mu^y)^\dagger]\psi_{\mathbf{k}}. \tag{7}$$

The subscripts X and Y correspond to the p_x and p_y structure, respectively. The f-wave spin-triplet Cooper pairs are described by

$$\vec{\Phi}_f(\mathbf{k}) = \psi^T_{-\mathbf{k}}[(-i\tau^y)(i\vec{\mu}\mu^y)^\dagger]\psi_{\mathbf{k}}. \tag{8}$$

In addition to the p wave and f wave, we find a *staggered* intrasublattice spin-triplet Cooper pair [34] given by

$$\vec{\Phi}_{\bar{s}}(\mathbf{k}) = \psi^T_{-\mathbf{k}}[(-i\tau^y)\sigma^z(i\vec{\mu}\mu^y)^\dagger]\psi_{\mathbf{k}}. \tag{9}$$

The σ^z indicates a staggered sublattice structure, which might suggest a vanishingly small effect, similar to the intravalley pairing terms.

The above bilinear exhaust all the possible spin-triplet pairing. We note that all the spin-triplet Cooper pairs discussed above can have a pairing potential with no explicit dependence on momentum $\mathbf{k}$. This should be

contrasted with other spin-triplet superconductors such as ^{3}He [29] and heavy fermion ferromagnetic superconductors [30,35], where the spin-triplet pairing potential is an odd function of momentum $\mathbf{k}$.

Notice that it is important to use the bilinear operators with respect to the basis in Eq. (1) because the expressions of Cooper pairs are basis dependent. We adopt the microscopic basis for Eq. (1) and the bilinear operators discussed above.

BCS theory.—To investigate the qualitative features of the superconductivity, we employ the standard BCS approach [29,36] and derive the pairing Hamiltonian from Eq. (5) (with the attractive channels only) as follows:

$$\hat{H}'_I = -\frac{\tilde{U}}{A}\sum_{\mathbf{k},\mathbf{k}'}{}'[\vec{\Phi}^\dagger_{p,X}(\mathbf{k})\cdot\vec{\Phi}_{p,X}(\mathbf{k}') + \vec{\Phi}^\dagger_{p,Y}(\mathbf{k})\cdot\vec{\Phi}_{p,Y}(\mathbf{k}') + \vec{\Phi}^\dagger_{\tilde{s}}(\mathbf{k})\cdot\vec{\Phi}_{\tilde{s}}(\mathbf{k}') + \vec{\Phi}^\dagger_{f}(\mathbf{k})\cdot\vec{\Phi}_{f}(\mathbf{k}')], \tag{10}$$

where $\tilde{U} > 0$ is the momentum-independent effective pairing strength, the prime in the momentum summation indicates summing half of the Brillouin zone. The interaction $\tilde{U}$ is momentum independent, but we still find unconventional pairings such as p wave and f wave because of the valley and sublattice degrees of freedom. $\tilde{U}$ can be derived from $\chi(\mathbf{q})$ in Eq. (5), which is discussed in Sec. II of [31]. Equation (10) describes attractive interactions among the spin-triplet Cooper pairs, implying spin-triplet superconductivity as the leading instability. The spin-singlet terms, which are left out in Eq. (10) are given in Sec. II of [31] and are checked to be repulsive as expected from ferromagnetic spin-fluctuation pairing [29].

To study the superconductivity, we employ the mean-field decoupling in Eq. (10) and express the mean field theory in terms of the Bogoliubov-de Gennes (BdG) Hamiltonian as follows:

$$\hat{H}_{\mathrm{MFT}} = \sum_{\mathbf{k}}{}'\Psi^\dagger_{\mathbf{k}}\mathcal{H}_{\mathrm{BdG}}(\mathbf{k})\Psi_{\mathbf{k}} + \frac{A}{\tilde{U}}(|\vec{\Delta}_{p,X}|^2 + |\vec{\Delta}_{p,Y}|^2 + |\vec{\Delta}_{f}|^2 + |\vec{\Delta}_{\tilde{s}}|^2), \tag{11}$$

where $\Psi^T_{\mathbf{k}} = [\psi^T_{\mathbf{k}}, \psi^\dagger_{-\mathbf{k}}(-i\mu^y)]$, $\vec{\Delta}_{p,X}$ ($\vec{\Delta}_{p,Y}$) is the order parameters for the p_x (p_y) pairing, and $\vec{\Delta}_f$ ($\vec{\Delta}_{\tilde{s}}$) is the order parameter for the f wave (staggered intrasublattice) pairing. $\mathcal{H}_{\mathrm{BdG}}(\mathbf{k})$ is expressed by

$$\mathcal{H}_{\mathrm{BdG}}(\mathbf{k}) = (\hbar v_F k_x)\sigma^x\tau^z\hat{1}_\kappa + (\hbar v_F k_y)\sigma^y\kappa^z - E_F\kappa^z + (\vec{\Xi}\cdot\vec{\mu})\kappa^+ + (\vec{\Xi}^\dagger\cdot\vec{\mu})\kappa^-, \tag{12}$$

$$\vec{\Xi} = \vec{\Delta}_{p,X}(-i\tau^y)\sigma^x + \vec{\Delta}_{p,Y}\tau^x(i\sigma^y) + \vec{\Delta}_f(-i\tau^y) + \vec{\Delta}_{\tilde{s}}(-i\tau^y)\sigma^z, \tag{13}$$

where the Pauli matrices ($\kappa^{x,y,z}$) and identity ($\hat{1}_\kappa$) in the particle-hole space are introduced and $\kappa^\pm = (\kappa^x \pm i\kappa^y)/2$. One can easily confirm the particle-hole symmetry

$$\hat{P}\mathcal{H}^*_{\mathrm{BdG}}(-\mathbf{k})\hat{P}^{-1} = -\mathcal{H}_{\mathrm{BdG}}(\mathbf{k}), \tag{14}$$

where $\hat{P} = \mu^y\kappa^y$, corresponding to the $\mathcal{P}^2 = 1$ particle-hole symmetry.

Formally, we can derive the free energy associated with Eq. (11) by integrating out the fermionic field in the partition function. Then, the free energy density ($\mathcal{F}$) is expressed by

$$\mathcal{F} = -\frac{k_B T}{A}\ln\det[-i\omega_n\hat{1} + \mathcal{H}_{\mathrm{BdG}}(\mathbf{k})] + \frac{1}{\tilde{U}}(|\vec{\Delta}_{\tilde{s}}|^2 + |\vec{\Delta}_{p,X}|^2 + |\vec{\Delta}_{p,Y}|^2 + |\vec{\Delta}_f|^2), \tag{15}$$

where k_B is the Boltzmann constant. We perform a perturbative expansion of $\mathcal{F}$ up to the quadratic order of the order parameter. This can be done systematically with the standard treatment in the matrix Green function approach [29]. The Landau-type free energy density is given by

$$\mathcal{F} = \mathrm{const} + \left[\frac{1}{\tilde{U}} - \xi(T)\right](|\vec{\Delta}_{p,X}|^2 + |\vec{\Delta}_{p,Y}|^2) + \left[\frac{1}{\tilde{U}} - \eta(T)\right]|\vec{\Delta}_f|^2 + \left[\frac{1}{\tilde{U}} - \zeta(T)\right]|\vec{\Delta}_{\tilde{s}}|^2 + O(|\Delta|^4), \tag{16}$$

where $\eta(T) > \xi(T) > \zeta(T) > 0$ (see Fig. 2 and Sec. IV in [31]), and T is the temperature. The transition temperatures can be determined by $\tilde{U}\xi(T_c^p) = 1$, $\tilde{U}\eta(T_c^f) = 1$, and $\tilde{U}\zeta(T_c^{\tilde{s}}) = 1$, where T_c^p, T_c^f, and $T_c^{\tilde{s}}$ are the transition temperatures for the p wave, f wave, and the

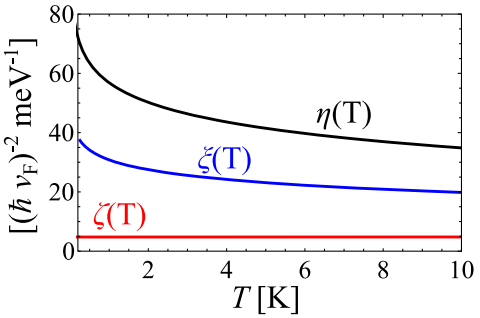

FIG. 2. Coefficients in the Landau free energy density. We plot $\eta(T)$ (black curve), $\xi(T)$ (blue curve), and $\zeta(T)$ (red curve) with $E_F = 30$ meV and $\hbar v_F\Lambda = 50$ meV. The unit in the y axis is $(\hbar v_F)^{-2}$ meV^{-1}. The results show that $\tilde{\eta}(T) > \tilde{\xi}(T) > \tilde{\zeta}(T)$ in the parameter regime relevant to MATTG experiment, suggesting that the f wave is the dominating pairing symmetry.

staggered intrasublattice spin-triplet pairings, respectively. Remarkably, we obtain that $T_c^f > T_c^p > T_c^s$, suggesting that the f wave is the dominating superconducting state. This result is due to the valley-sublattice structure [32,33] (see Sec. IV in [31] for a discussion) rather than the detail band structure, and we anticipate that the f wave is generically the dominating pairing symmetry for spin-triplet superconductivity in the graphene based systems including MATTG, independent of the pairing mechanism. We note that the possibility of realizing f-wave superconductivity was also discussed previously in the context of graphene and MATBG [33,37–43].

f-wave superconductivity.—In the rest of this Letter, we focus on the f-wave pairing spin-triplet superconductivity. With only the f-wave order parameter, the free energy density given by Eq. (15) can be derived exactly (see Sec. V of [31]) and is expressed by

$$\mathcal{F} = -2k_BT\sum_{s,r=\pm}\int_{\mathbf{k}} \ln\left[2\cosh\left(\frac{\sqrt{\epsilon_{\mathbf{k},s}^2+\Delta_r^2}}{2k_BT}\right)\right] + \frac{|\vec{\Delta}_f|^2}{\tilde{U}}, \tag{17}$$

where $\epsilon_{\mathbf{k},\pm} = \hbar v_F|\mathbf{k}| \pm E_F$, $\Delta_\pm = \sqrt{|\vec{\Delta}_f|^2 \pm |i\vec{\Delta}_f \times \vec{\Delta}_f^*|}$, and $\int_{\mathbf{k}}$ denotes $\int[d^2\mathbf{k}/(2\pi)^2]$. Without a magnetic field, the free energy is minimized when $i\vec{\Delta}_f \times \vec{\Delta}_f^* = 0$ (i.e., $\vec{\Delta}_f \| \vec{\Delta}_f^*$). Therefore, the order parameter can be expressed by $\vec{\Delta}_f = e^{i\phi}\vec{O}$, where $\vec{O}$ is a real-valued vector. Note that the phase ϕ can be gauged away. We find that the f wave BdG Hamiltonian satisfies a ($\mathcal{T}^2 = 1$) time-reversal symmetry:

$$\hat{\Pi}\mathcal{H}_{\mathrm{BdG}}^*(-\mathbf{k})\hat{\Pi}^{-1} = \mathcal{H}_{\mathrm{BdG}}(\mathbf{k}), \tag{18}$$

where $\hat{\Pi} = \sigma^y\tau^z\mu^y$ [44]. The superconducting state here belongs to the class BDI, which is topologically trivial in two dimensions based on the tenfold way classification [45]. As such, we conclude that the spin-triplet f-wave pairing superconducting state is *unitary* (i.e., $i\vec{\Delta}_f \times \vec{\Delta}_f^* = 0$), time-reversal symmetric, fully gapped, and topologically trivial.

To derive the gap equation, we minimize the free energy in Eq. (17) with respect to $|\vec{\Delta}_f|^2$ (with $i\vec{\Delta}_f \times \vec{\Delta}_f^* = 0$). The gap equation is expressed by

$$\frac{1}{\tilde{U}} = \int_{\mathbf{k}}\left[\frac{\tanh(\frac{E_{\mathbf{k},+}}{2k_BT})}{E_{\mathbf{k},+}} + \frac{\tanh(\frac{E_{\mathbf{k},-}}{2k_BT})}{E_{\mathbf{k},-}}\right], \tag{19}$$

where $E_{\mathbf{k},\pm} = \sqrt{\epsilon_{\mathbf{k},\pm}^2 + |\vec{\Delta}_f|^2}$. To regularize the momentum space integral, we introduce a momentum cutoff (Λ). For $|\vec{\Delta}_f| \ll |E_F|$, $\hbar v_F\Lambda$, we derive the asymptotic expressions for the zero temperature gap, $2\Delta_0 \equiv 2|\vec{\Delta}_f(T=0)|$, and the transition temperature, T_c^f, as follows [46]:

$$2\Delta_0 = 2|E_F|\mathcal{A}\exp\left[-\frac{1}{\tilde{U}N(E_F)}\right], \tag{20}$$

$$k_BT_c^f = |E_F|\frac{e^\gamma}{\pi}\mathcal{A}\exp\left[-\frac{1}{\tilde{U}N(E_F)}\right], \tag{21}$$

where $\mathcal{A} = 2\sqrt{[(\hbar v_F\Lambda - |E_F|)/(\hbar v_F\Lambda + |E_F|)]}\times \exp\left[(\hbar v_F\Lambda - |E_F|)/|E_F|\right]$ is a dimensionless parameter, γ is the Euler-Mascheroni constant, and $N(E_F) = |E_F|/(2\pi\hbar^2 v_F^2)$ is the density of states at the Fermi energy.

To gain an intuitive understanding, we expand the free energy density (without an applied magnetic field) in Eq. (17) up to the quartic order of the order parameter as follows:

$$\mathcal{F} = \mathrm{const} + \sum_{a=x,y,z}\left[\frac{2}{g^2U} - \eta_a(T)\right]|\Delta_f^a|^2 + a_4(T)[|\vec{\Delta}_f|^4 + |i\vec{\Delta}_f^* \times \vec{\Delta}_f|^2] + O(|\Delta_f|^6), \tag{22}$$

where $a_4(T) > 0$ and $\eta_a(T) = \eta(T)$ in the absence of a magnetic field. The absence of $i\vec{\Delta}_f \times \vec{\Delta}_f^*$ is the manifestation of the positive $a_4(T)$ in the Landau theory.

In the presence of a small in-plane magnetic field, the electronic band develops a Zeeman splitting. Then, $-B\mu^z$ is added to $h_{\mathbf{k}}$ [Eq. (2)], where $2B$ denotes the Zeeman splitting and the z direction is rotated to the field direction. Similar to the expansion in Eq. (16), we treat the order parameter perturbatively. In addition, we also treat $-B\mu^z$ perturbatively in the Green functions. (See Sec. VI of [31] for a derivation.) The free energy density acquires a term proportional to $-iB\vec{\Delta}_f \times \vec{\Delta}_f^* \cdot \hat{z}$, implying $i\vec{\Delta}_f \times \vec{\Delta}_f^* \cdot \hat{z} \neq 0$ and a finite magnetization in the superconducting state. The quadratic terms in the free energy density are also affected by B as illustrated in Fig. 3. Specifically, $\eta_x(T,B) = \eta_y(T,B) = \eta(T,0) + B^2\delta\eta(T)$ and $\eta_z(T,B) = \eta(T,0) - B^2\delta\eta(T)$, where $\delta\eta(T) > 0$ (Sec. VI of [31]). Thus, Δ_f^x and Δ_f^y are the favored states, suggesting that equal-spin pairing is the dominating pairing structure with a Zeeman splitting [See Eq. (8)]. Recall that

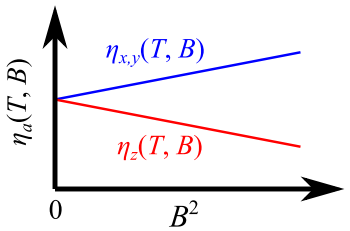

FIG. 3. Sketch of $\eta_a(T,B)$ versus B^2. In the absence of Zeeman splitting (i.e., $B=0$), $\eta_x(T,0) = \eta_y(T,0) = \eta_z(T,0)$. For a small finite B, $\eta_x(T,B) = \eta_y(T,B) > \eta_z(T,B)$ and $\eta_x(T,B) - \eta_z(T,B) \propto B^2$. See main text for a detailed discussion.

$\Delta_\pm = \sqrt{|\vec{\Delta}_f|^2 \pm |i\vec{\Delta}_f \times \vec{\Delta}_f^*|}$. Thus, there are two gaps in the superconducting state. For a small B, the gap formed by "up" spins is increased while the gap formed by the "down" spins is suppressed. This is consistent with the previous theoretical results in [47] for MATBG. We conclude that the superconductivity with a small in-plane field is f wave, spin-triplet, and equal-spin pairing.

Relation to MATTG experiment.—A recent MATTG experiment found that the superconductivity near $\nu = -2$ persists for a large magnetic field (10 T) beyond the Pauli limit for the spin-singlet superconductivity [21]. A natural explanation is that the superconductivity is spin-triplet, which we emphasize in this Letter. However, there is no clear sign of magnetism in the experiments. A possible explanation is that the electrons are spin polarized, but the coherence length is too small to develop a true long-range order. In such a scenario, the phenomenological spin-fermion model provides a natural starting point. In addition, our predicted f-wave superconducting state can withstand finite Zeeman splitting, and the gap (from the up spins) is enhanced for a small in-plane magnetic field. To compare with the MATTG experiments, we take $v_F = 4 \times 10^4$ m/s, $\hbar v_F \Lambda = 50$ meV (half of the MATTG bandwidth [19]), $|E_F| = 30$ meV, and $\tilde{U} = 30\ \mathrm{meV\,nm^2}$. Putting these numbers in Eq. (21), we obtain $T_c^f = 3$ K, which is comparable to the extracted T_{BKT} in the experiments [19,20]. We also note that $\tilde{U}$ cannot be larger than $\tilde{U}_c \sim 1/\rho_0$ (with ρ_0 being the density of states at Fermi level) as the Stoner ferromagnetism must be absent in the normal state. Although the spin-fluctuation mechanism proposed in this work is likely, we cannot not rule out the acoustic-phonon mechanism which might realize f-wave spin-triplet superconductivity also [33,48,49].

The f-wave spin-triplet superconductivity can be examined experimentally. The spin-triplet Cooper pair cannot tunnel into a spin-singlet superconductor (i.e., zero Josephson current) but can tunnel into an "Ising" superconductor (such as $NbSe_2$ [50,51]) as long as the spin-triplet Cooper pair has zero out-of-plane spin projection. Since the small magnetic field can partially polarize the superconducting state, the MATTG-$NbSe_2$ junction with a small magnetic field can distinguish the spin-triplet pairing from the spin-singlet pairing. In addition, the f-wave symmetry can be confirmed by a hybrid corner Josephson junction as discussed in Sec. VII of [31].

Relation to the Hubbard model.—The phenomenological spin-fermion model used in this work might be derived from the Hubbard model [27]. In the single-band square lattice $SU(2)$ Hubbard model, the antiferromagnetism arises at half filling for a large on-site repulsion, and the Nagaoka ferromagnetism takes place when doping slightly away from the half filling. We expect that the phenomenological spin-fermion model here should capture the gross features of the possible spin polarized states in the MATTG bands. However, the microscopic justification remains an important question, both whether there is superconductivity in the Hubbard model [52] and whether the Hubbard model is relevant to MATTG [43,53,54]. Our work, however, transcends these questions and applies as long as spin fluctuations mediate the observed superconductivity.

Outlook.—The present work can be straightforwardly generalized to the MATTG bands [55–57], which is an important direction for future work. We anticipate that the f wave remains the main pairing symmetry because of the valley-sublattice structure unique to graphene. In this Letter, we concentrate only on the zero and the low in-plane magnetic field limits. With a sufficiently large in-plane magnetic field, the spin fields are fully polarized, and a sizable Zeeman splitting in the electronic bands develops. The transverse fluctuation of the polarized spin fields (analogous to the magnon) can still mediate the effective interaction. The presence of spin fluctuations implies that the Pomenranchauk effect applies to the system [58,59].

We are grateful to Andrey Chubukov, Pablo Jarillo-Herrero, and Andrea Young for stimulating correspondence. Y.-Z. C. also thanks Zhentao Wang for useful discussions. This work is supported by the Laboratory for Physical Sciences (Y.-Z. C. and S. D. S.), by JQI-NSF-PFC (supported by NSF Grant No. PHY-1607611, Y.-Z. C.), and NSF DMR1555135 (CAREER, J. D. S.). F. W. is supported by startup funding of Wuhan University.

*yzchou@umd.edu

[1] Y. Cao, V. Fatemi, A. Demir, S. Fang, S. L. Tomarken, J. Y. Luo, J. D. Sanchez-Yamagishi, K. Watanabe, T. Taniguchi, E. Kaxiras *et al.*, Nature (London) **556**, 80 (2018).
[2] Y. Cao, V. Fatemi, S. Fang, K. Watanabe, T. Taniguchi, E. Kaxiras, and P. Jarillo-Herrero, Nature (London) **556**, 43 (2018).
[3] M. Yankowitz, S. Chen, H. Polshyn, Y. Zhang, K. Watanabe, T. Taniguchi, D. Graf, A. F. Young, and C. R. Dean, Science **363**, 1059 (2019).
[4] H. Polshyn, M. Yankowitz, S. Chen, Y. Zhang, K. Watanabe, T. Taniguchi, C. R. Dean, and A. F. Young, Nat. Phys. **15**, 1011 (2019).
[5] Y. Cao, D. Chowdhury, D. Rodan-Legrain, O. Rubies-Bigorda, K. Watanabe, T. Taniguchi, T. Senthil, and P. Jarillo-Herrero, Phys. Rev. Lett. **124**, 076801 (2020).
[6] A. L. Sharpe, E. J. Fox, A. W. Barnard, J. Finney, K. Watanabe, T. Taniguchi, M. Kastner, and D. Goldhaber-Gordon, Science **365**, 605 (2019).
[7] X. Lu, P. Stepanov, W. Yang, M. Xie, M. A. Aamir, I. Das, C. Urgell, K. Watanabe, T. Taniguchi, G. Zhang *et al.*, Nature (London) **574**, 653 (2019).
[8] A. Kerelsky, L. J. McGilly, D. M. Kennes, L. Xian, M. Yankowitz, S. Chen, K. Watanabe, T. Taniguchi, J. Hone, C. Dean *et al.*, Nature (London) **572**, 95 (2019).
[9] Y. Jiang, X. Lai, K. Watanabe, T. Taniguchi, K. Haule, J. Mao, and E. Y. Andrei, Nature (London) **573**, 91 (2019).

[10] Y. Xie, B. Lian, B. Jäck, X. Liu, C.-L. Chiu, K. Watanabe, T. Taniguchi, B. A. Bernevig, and A. Yazdani, Nature (London) **572**, 101 (2019).

[11] Y. Choi, J. Kemmer, Y. Peng, A. Thomson, H. Arora, R. Polski, Y. Zhang, H. Ren, J. Alicea, G. Refael *et al.*, Nat. Phys. **15**, 1174 (2019).

[12] M. Serlin, C. Tschirhart, H. Polshyn, Y. Zhang, J. Zhu, K. Watanabe, T. Taniguchi, L. Balents, and A. Young, Science **367**, 900 (2020).

[13] J. M. Park, Y. Cao, K. Watanabe, T. Taniguchi, and P. Jarillo-Herrero, Nature (London) **592**, 43 (2021).

[14] G. Chen, A. L. Sharpe, P. Gallagher, I. T. Rosen, E. J. Fox, L. Jiang, B. Lyu, H. Li, K. Watanabe, T. Taniguchi *et al.*, Nature (London) **572**, 215 (2019).

[15] G. W. Burg, J. Zhu, T. Taniguchi, K. Watanabe, A. H. MacDonald, and E. Tutuc, Phys. Rev. Lett. **123**, 197702 (2019).

[16] C. Shen, Y. Chu, Q. Wu, N. Li, S. Wang, Y. Zhao, J. Tang, J. Liu, J. Tian, K. Watanabe *et al.*, Nat. Phys. **16**, 520 (2020).

[17] Y. Cao, D. Rodan-Legrain, O. Rubies-Bigorda, J. M. Park, K. Watanabe, T. Taniguchi, and P. Jarillo-Herrero, Nature (London) **583**, 215 (2020).

[18] X. Liu, Z. Hao, E. Khalaf, J. Y. Lee, Y. Ronen, H. Yoo, D. H. Najafabadi, K. Watanabe, T. Taniguchi, A. Vishwanath *et al.*, Nature (London) **583**, 221 (2020).

[19] J. M. Park, Y. Cao, K. Watanabe, T. Taniguchi, and P. Jarillo-Herrero, Nature (London) **590**, 249 (2021).

[20] Z. Hao, A. Zimmerman, P. Ledwith, E. Khalaf, D. H. Najafabadi, K. Watanabe, T. Taniguchi, A. Vishwanath, and P. Kim, Science **371**, 1133 (2021).

[21] Y. Cao, J. M. Park, K. Watanabe, T. Taniguchi, and P. Jarillo-Herrero, Nature (London) **595**, 526 (2021).

[22] P. Monthoux and G. G. Lonzarich, Phys. Rev. B **59**, 14598 (1999).

[23] K. B. Blagoev, J. R. Engelbrecht, and K. S. Bedell, Phys. Rev. Lett. **82**, 133 (1999).

[24] R. Roussev and A. J. Millis, Phys. Rev. B **63**, 140504(R) (2001).

[25] A. Abanov, A. V. Chubukov, and A. Finkel'stein, Europhys. Lett. **54**, 488 (2001).

[26] A. V. Chubukov, A. M. Finkel'stein, R. Haslinger, and D. K. Morr, Phys. Rev. Lett. **90**, 077002 (2003).

[27] A. Abanov, A. V. Chubukov, and J. Schmalian, Adv. Phys. **52**, 119 (2003).

[28] F. Wu, Phys. Rev. B **99**, 195114 (2019).

[29] P. Coleman, *Introduction to Many-Body Physics* (Cambridge University Press, Cambridge, England, 2015), ISBN: v9780521864886.

[30] V. P. Mineev, Phys. Usp. **60**, 121 (2017).

[31] See Supplemental Material at http://link.aps.org/supplemental/10.1103/PhysRevLett.127.217001 for some technical details for the main results in main text.

[32] F. Wu, A. H. MacDonald, and I. Martin, Phys. Rev. Lett. **121**, 257001 (2018).

[33] F. Wu, E. Hwang, and S. Das Sarma, Phys. Rev. B **99**, 165112 (2019).

[34] This pairing can be derived from the f-wave state as the difference is a σ^z in the expression. The $\mathcal{C}_{2z}$ and $\mathcal{C}_{3z}$ operations are consistent with s wave, but this is not the conventional s-wave state due to the staggered sublattice structure.

[35] S. Ran, C. Eckberg, Q.-P. Ding, Y. Furukawa, T. Metz, S. R. Saha, I.-L. Liu, M. Zic, H. Kim, J. Paglione *et al.*, Science **365**, 684 (2019).

[36] K. V. Samokhin and V. P. Mineev, Phys. Rev. B **77**, 104520 (2008).

[37] R. Nandkishore, R. Thomale, and A. V. Chubukov, Phys. Rev. B **89**, 144501 (2014).

[38] Y.-P. Lin and R. M. Nandkishore, Phys. Rev. B **98**, 214521 (2018).

[39] X. Wu, W. Hanke, M. Fink, M. Klett, and R. Thomale, Phys. Rev. B **101**, 134517 (2020).

[40] Y. Wang, J. Kang, and R. M. Fernandes, Phys. Rev. B **103**, 024506 (2021).

[41] R. E. Throckmorton and S. Das Sarma, Phys. Rev. Research **2**, 023225 (2020).

[42] M. Alidoust, M. Willatzen, and A.-P. Jauho, Phys. Rev. B **99**, 155413 (2019).

[43] A. L. Szabó and B. Roy, Phys. Rev. B **103**, 205135 (2021).

[44] Formally, $\hat{\Pi} = \tau^x \mu^y$, corresponding to $\mathcal{T}^2 = -1$, is the physical time-reversal symmetry. The existence of $\mathcal{T}^2 = 1$ time-reversal operation is resulted from the spin-conservation. Thus, the irreducible diagonal block Hamiltonian should be viewed as a system with effectively $\mathcal{T}^2 = 1$.

[45] A. P. Schnyder, S. Ryu, A. Furusaki, and A. W. W. Ludwig, Phys. Rev. B **78**, 195125 (2008).

[46] We note that Eqs. (21) and (21) fail when $E_F = 0$ (Dirac point), which is in fact an unstable non-Fermi-liquid fixed point, indicating the breakdown of BCS theory without a finite Fermi surface.

[47] F. Wu and S. Das Sarma, Phys. Rev. B **99**, 220507(R) (2019).

[48] F. Wu and S. Das Sarma, Phys. Rev. B **101**, 155149 (2020).

[49] Y.-Z. Chou, F. Wu, J. D. Sau, and S. Das Sarma, Phys. Rev. Lett. **127**, 187001 (2021).

[50] X. Xi, Z. Wang, W. Zhao, J.-H. Park, K. T. Law, H. Berger, L. Forró, J. Shan, and K. F. Mak, Nat. Phys. **12**, 139 (2016).

[51] M. Kim, G.-H. Park, J. Lee, J. H. Lee, J. Park, H. Lee, G.-H. Lee, and H.-J. Lee, Nano Lett. **17**, 6125 (2017).

[52] D. P. Arovas, E. Berg, S. Kivelson, and S. Raghu, arXiv:2103.12097.

[53] A. Fischer, Z. A. Goodwin, A. A. Mostofi, J. Lischner, D. M. Kennes, and L. Klebl, arXiv:2104.10176.

[54] B. Roy and V. Juričić, Phys. Rev. B **99**, 121407(R) (2019).

[55] X. Li, F. Wu, and A. H. MacDonald, arXiv:1907.12338.

[56] E. Khalaf, A. J. Kruchkov, G. Tarnopolsky, and A. Vishwanath, Phys. Rev. B **100**, 085109 (2019).

[57] D. Călugăru, F. Xie, Z.-D. Song, B. Lian, N. Regnault, and B. A. Bernevig, Phys. Rev. B **103**, 195411 (2021).

[58] A. Rozen, J. M. Park, U. Zondiner, Y. Cao, D. Rodan-Legrain, T. Taniguchi, K. Watanabe, Y. Oreg, A. Stern, E. Berg *et al.*, Nature (London) **592**, 214 (2021).

[59] Y. Saito, F. Yang, J. Ge, X. Liu, T. Taniguchi, K. Watanabe, J. Li, E. Berg, and A. F. Young, Nature (London) **592**, 220 (2021).